KAPL-P-000194
(K97127)
CONF-971201--

SUBSTRATE MISORIENTATION EFFECTS ON EPITAXIAL GaInAsSb

G. W. Charache, C. A. Wang, et. al.

December 1997

NOTICE

KAPL ATOMIC POWER LABORATORY SCHENECTADY, NEW YORK 10701

Operated for the U. S. Department of Energy
by KAPL, Inc. a Lockheed Martin company

DISCLAIMER

DISCLAIMER

Portions of this document may be illegible in electronic image products. Images are produced from the best available original document.

MS-12-488

Substrate Misorientation Effects on Epitaxial GaInAsSb *

C.A. Wang, H.K. Choi, and D.C. Oakley
Lincoln Laboratory, Massachusetts Institute of Technology, Lexington, MA 02173-9108

G.W. Charache, Lockheed Martin Corporation, Schenectady, NY 12301

ABSTRACT

The effect of substrate misorientation on the growth of GaInAsSb was studied for epilayers grown lattice-matched to GaSb substrates by low-pressure organometallic vapor phase epitaxy. The substrates were (100) misoriented 2 or 6° toward (110), (111)A, or (111)B. The surface is mirror-like and featureless for layers grown with a 6° toward (111)B misorientation, while, a slight texture was observed for layers grown on all other misorientations. The optical quality of layers, as determined by the full width at half-maximum of photoluminescence spectra measured at 4K, is significantly better for layers grown on substrates with a 6° toward (111)B misorientation. The incorporation of Zn as a p-type dopant in GaInAsSb is about 1.5 times more efficient on substrates with 6° toward (111)B misorientation compared to 2° toward (110) misorientation. The external quantum efficiency of thermophotovoltaic devices is not, however, significantly affected by substrate misorientation.

INTRODUCTION

$Ga_{1-x}In_xAs_ySb_{1-y}$ is an important material for optoelectronic devices that operate in the mid-infrared. This alloy can be lattice matched to GaSb or InAs susbtrates and has a direct energy gap adjustable in the wavelength range from 1.7 (0.726 eV) to 4.2 μm (0.296 eV). Although most quaternary alloy compositions are predicted to exhibit thermodynamic immiscibility at typical growth temperatures [1,2], stable alloys with a cutoff wavelength of 2.39 μm were grown by liquid phase epitaxy (LPE) [3], and metastable alloys were grown by organometallic vapor phase epitaxy (OMVPE) [4] and molecular beam epitaxy (MBE) [5]. Devices that include lasers [6,7], photodetectors [8], and thermophotovoltaic devices [9,10] have been reported, and the technological interest of GaInAsSb continues to increase.

The growth of GaInAsSb has been performed, in general, on nominally (100) oriented GaSb substrates. The use of vicinal substrates for the growth of III-V semiconductors, however, can play an important role in the resulting material quality. For example, the surface

*This work was sponsored by the Department of Energy under AF Contract No. F19628-95-C-0002. The opinions, interpretations, conclusions and recommendations are those of the author and are not necessarily endorsed by the United States Air Force.

morphology of GaAs layers was reported to be smoother for OMVPE growth on (100) substrates with a 2° misorientation toward (110) [11], and higher optical quality of MBE-grown GaAs/AlGaAs quantum wells was observed on vicinal substrates [12]. Furthermore, the device performance of GaAs/AlGaAs quantum-well lasers was significantly improved on tilted substrates [13]. In this paper, we report the growth and material characteristics of GaInAsSb alloys lattice matched to vicinal GaSb substrates with misorientations of 2 and 6° off (100) substrates toward (110), (111)A, and (111)B. The best surface morphology and highest optical quality are obtained for substrates with a 6° toward (111)B misorientation. The performance of thermophotovoltaic devices grown on (100) GaSb substrates with either a 2° toward (110) or 6° toward (111)B misorientation are compared.

EPITAXIAL GROWTH AND CHARACTERIZATION

$Ga_{1-x}In_xAs_ySb_{1-y}$ epilayers were grown in a vertical rotating-disk reactor with H_2 carrier gas at a flow rate of 10 slpm and reactor pressure of 150 Torr [14]. Solution trimethylindium, triethylgallium, tertiarybutylarsine, and trimethylantimony were used as organometallic sources. The growth rate was typically 2.5 μm/hr. The V/III ratio ranged from 1.1 to 1.3 and the growth temperature ranged from 525 - 575°C. For doping studies, diethyltellurium (DETe) (50 ppm in H_2) and dimethylzinc (DMZn) (1000 ppm in H_2) were used as n- and p-type doping sources, respectively.

GaInAsSb was grown on (100) Te-doped GaSb substrates with misorientation angles of either 2 or 6° toward (110), (111)A or (111)B. For direct comparison, epilayers were grown side-by-side on substrates of various misorientation angles to minimize the effects of run-to-run variability. The surface morphology was examined using Nomarski contrast microscopy. Double-crystal x-ray diffraction (DCXD) was used to measure the degree of lattice mismatch to GaSb substrates. Photoluminescence (PL) was measured at 4 and 300K using a PbS detector. The composition of epilayers was determined from DCXD splitting, the peak emission in PL spectra, and the energy gap dependence on composition based on the binary bandgaps as

described in a previous reference [14]. For electrical characterization, GaInAsSb was grown on semi-insulating (SI) (100) GaAs substrates misoriented 2° toward (110) or 6° toward (111)B. Carrier concentration and mobility were obtained from Hall measurements based on the van der Pauw method.

RESULTS

The surface morphology of $Ga_{1-x}In_xAs_ySb_{1-y}$ layers grown at 550°C on vicinal GaSb substrates is shown in Figs. 1a-f. The Nomarski interference micrographs correspond to layers grown on (100) substrates with a 2 or 6° misorientation toward (110), (111)A, and (111)B, respectively. The composition of these layers is x=0.18 and y=0.15 and corresponds to 300K PL peak emission at ~2.4 μm. The layers grown on substrates with a 2° misorientation exhibit considerable texture. A smoother surface morphology is observed for layers grown on substrates with a 6° misorientation, and the smoothest surface is observed for 6° toward (111)B misorientation.

On the other hand, the dependence of GaInAsSb surface morphology on substrate misorientation is less sensitive as the In concentration is decreased (i.e., composition moving away from immiscibility gap). For x~0.1, y~0.08 (~2.1 μm cutoff at room temperature), smooth $Ga_{1-x}In_xAs_ySb_{1-y}$ surfaces could be obtained for epilayers grown at a growth temperature of 550°C and with 2° misorientation toward (110). Other factors that affect the surface morphology are the growth temperature and V/III ratio. In general, for layers with similar composition, a smoother morphology is observed for those layers grown at lower temperatures. We also observed that the surface texture of layers with a 2° toward (110) misorientation increased when the V/III ratio was increased above the minimum value for stoichiometric GaInAsSb. In contrast, the 6° toward (111)B misorientation was less sensitive. These observations suggest that the 6° toward (111)B misorientation provides a wider operating range of growth parameters for which a smooth morphology can be obtained.

Since the (100) 2° toward (110) substrate is widely used for OMVPE growth, subsequent comparisons are made for layers grown on either (100) 2° toward (110) or (100) 6° toward (111)B substrates. The 4K PL spectra also show striking differences that depend on substrate misorientation. Figure 2 shows the PL spectra for GaInAsSb grown at 550°C. The full width at half-maximum (FWHM) for the 2° misorientation is 15.4 meV compared to a FWHM value of 7.5 meV for the 6° misorientation. In addition, the peak emission is longer at 2045 nm for the 2° misorientation compared to 1995 nm for the 6° misorientation. Data for 4K FWHM of layers of different In composition and grown at 550 or 525°C are shown in Fig. 3, and plotted versus the PL peak position. Over the whole range, the FWHM value is consistently lower for the 6° misorientation. In addition, the PL peak position is at higher energy indicating a lower In incorporation. A dependence of In incorporation on substrate misorientation has also been reported for InGaAs [15]. The data in Fig. 3 also indicate that the PL FWHM is dependent on the growth temperature. A smaller difference in FWHM is observed for layers grown at 525°C compared to those at 550°C.

Figure 4 summarizes our best FWHM data for GaInAsSb epilayers. These samples were grown at 550°C on (100) 6° toward (111)B substrates or at 525°C on either (100) 2° toward (110) or 6° toward (111)B substrates. Also shown for comparison are data for layers grown by OMVPE on (100) substrates [16,17]. The FWHM values for samples in this study are significantly smaller than those reported previously, especially at the lower PL peak energy. The smallest FWHM value measured is 7.1 meV at 0.606 eV (2047 nm). The corresponding peak energy at 300K for this sample is 0.547 eV (2267 nm). Our FWHM values are comparable to those reported for layers grown by MBE [18]. For GaInAsSb grown by LPE, a FWHM value of 9 meV at 0.587 eV (2112 nm) was reported [19].

The p- and n-doping of GaInAsSb is also dependent on the substrate misorientation. Figures 5 and 6 show the hole and electron concentration versus the dopant mole fraction in the

gas phase, respectively, for the 2° toward (110) and 6° toward (111)B misorientations. These layers were grown at 550°C on a 0.4 μm-thick undoped GaSb buffer layer, which has been shown to reduce the contribution of electrically active defects due to the lattice mismatch between the GaInAsSb and the SI GaAs substrate [18]. For p-GaInAsSb, the hole concentration ranges from 6.3 x 10^{16} to 1.7 x 10^{18} cm^{-3}. It is 1.5 to 1.6 times greater for the layers grown with a 6° toward (111)B misorientation compared to the 2° toward (110) misorientation. These results suggest that there is a preferential incorporation of Zn for the 6° toward (111)B misorientation. For n-GaInAsSb, the electron concentration ranges from 2.3 x 10^{17} to 2.3 x 10^{18} cm^{-3}, and is 0.86 to 0.9 times lower for the 6° toward (111)B misorientation compared to the 2° toward (110) misorientation.

To investigate the effect of substrate misorientation on the performance of thermophotovoltaic devices, structures were grown on (100) n-GaSb substrates with a 2° toward (110) or 6° toward (111)B misorientation. The structure consists of 1-μm-thick n-GaInAsSb, 5-μm-thick p-GaInAsSb, 0.1-μm-thick p-AlGaAsSb, and 0.05-μm-thick p-GaSb. For this comparison, the structures were grown in two separate growth runs. The growth temperature was 550°C. Mesa diodes, 1 cm^2, were fabricated by a conventional photolithographic process. Ohmic contacts to p- and n-GaSb were formed by depositing Ti/Pt/Au and Au/Sn/Ti/Pt/Au, respectively, and alloying at 300°C. A single 1-mm-wide central busbar connected to the 10-μm-wide grid lines spaced 100 μm apart was used to make electrical contact to the front surface.

The external quantum efficiency (QE) versus wavelength for the two devices is shown in Fig. 7. Surprisingly, the QE of the devices grown on the two misorientations are comparable, with only a slightly higher QE measured for the device grown with the 6° misorientation. Since the QE is highly dependent on the minority carrier lifetime, this result suggests that the lifetime is less affected by substrate misorientation. The cutoff wavelength for the device grown on (100) 6° toward (111)B is longer. This is a result of the gas flows used to grow the structure, and not a consequence of the misorientation angle.

CONCLUSIONS

The quality of GaInAsSb epilayers grown by OMVPE is dependent on the substrate misorientation, especially for alloy compositions approaching the immiscibility boundary. A smoother surface morphology and narrower PL FWHM was observed for layers grown on (100) substrates with a 6° toward (111)B misorientation compared to that grown on (100) 2° toward (110) substrates. These effects of substrate misorientation can be minimized by growing the layers at lower temperatures. However, for the growth of device structures that include other Sb-based alloys such as AlGaAsSb, higher growth temperatures may be more desirable. Consequently, the use of (100) substrates with a 6° toward (111)B misorientation will allow a wider growth operating window, and subsequently will provide more consistent results. It was also found that the performance of thermophotovoltaic devices is less sensitive to the substrate misorientation.

ACKNOWLEDGMENTS

The authors gratefully acknowledge D.R. Calawa, J.W. Chludzinski, M.K. Connors, and V. Todman-Bams for technical assistance, K.J. Challberg for manuscript editing, and D.L. Spears for continued support and encouragement.

REFERENCES

1. K. Onabe, Jpn. J. Appl. Phys. **21**, 964 (1982).
2. G.B. Stringfellow, J. Cryst. Growth **58**, 194 (1982).
3. E. Tournie, F. Pitard, and A. Joullie, J. Cryst. Growth **104**, 683 (1990).
4. M.J. Cherng, H.R. Jen, C.A. Larsen, G.B. Stringfellow, H. Lundt, and P.C. Taylor, J. Cryst. Growth **77**, 408 (1986).
5. H.K. Choi, S.J. Eglash, and G.W. Turner, Appl. Phys. Lett. **64**, 2474 (1994).
6. D.Z. Garbuzov, R.U. Martinelli, H. Lee, P.K. York, R.J. Menna, J.C. Connolly and S.Y. Narayan, Appl. Phys. Lett. **69**, 2006 (1996).
7. H.K. Choi, G.W. Turner, M.K. Connors, S. Fox, C. Dauga, and M. Dagenais, IEEE Photon. Tech. Lett. **7**, 281 (1995).

8. Y. Shi, J.H. Zhao, H. Lee, J. Sarathy, M. Cohen, and G. Olsen, Electron. Lett. **32**, 2268 (1996).

9. P.N. Uppal, G. Chrarache, P. Baldasaro, B. Campbell, S. Loughin, S. Svensson, and D. Gill, J. Cryst. Growth **175/176**, 877 (1997).

10. C.A. Wang, H.K. Choi, G.W. Turner, D.L. Spears, M.J. Manfra, and G.W. Charache, 3rd NREL Conference on the Thermophotovoltaic Generation of Electricity, edited by J.P. Benner and T.J. Coutts, AIP Conf. Proc. **401**, Woodbury, NY, 1997, p. 75.

11. M. Mizuta, S. Kawata, T. Iwamoto, and H. Hiroshi, Jap. J. Appl. Phys. **5**, L283 (1984).

12. R.K. Tsui, G.D. Kramer, J.A. Curless, and M.S. Peffley, Appl. Phus. Lett. **48**, 940 (1986).

13. H.Z. Chen, A. Ghaffari, H. Morkoc, and A. Yariv, Appl. Phys. Lett. **51**, 2094 (1987).

14. C.A. Wang and H.K. Choi, to appear J. Electron. Mater.

15. J. tc Nijenhuis, P.R. Hageman, and L.J. Giling, J. Cryst. Growth **167**, 397 (1996).

16. M. Sopanen, T. Koljonen, H. Lipsanen, and T. Tuomi, J. Cryst. Growth **145**, 492 (1994).

17. J.Shin, T.C. Hsu, Y. Hsu, and G.B. Stringfellow, J. Cryst. Growth **179**, 1 (1997).

18. C.A. Wang, G.W. Turner, M.J. Manfra, H.K. Choi, and D.L. Spears, Mat. Res. Soc. Symp. Proc. Vol. 450, 55 (1997).

19. E. Tournie, J.-L. Lazzari, F. Pitard, C. Alibert, A. Joullie, and B. Lambert, J. Appl. Phys. **68**, 5936 (1990).

FIGURE CAPTIONS

Figure 1 Surface morphology of $Ga_{0.82}In_{0.18}As_{0.15}Sb_{0.85}$ epilayers grown on GaSb substrates at 550°C and various substrate misorientations.

Figure 2 Photoluminescence spectra measured at 4K of GaInAsSb grown on (100) GaSb with (a) 2° toward (110) and (b) 6° toward (111)B misorientations.

Figure 3 Photoluminescence FWHM measured at 4K of GaInAsSb grown on (100) GaSb with a 2° toward (110) (closed symbols) and 6° toward (111)B misorientations (open symbols) at 525° C (triangles) and 550°C (circles).

Figure 4 Photoluminescence FWHM measured at 4K of GaInAsSb layers grown on GaSb substrates. Solid circles this work; open squares from reference 16; open triangles from reference 17.

Figure 5 Hole concentration measured at 300K of p-GaInAsSb as a function of DMZn mole fraction grown on (100) semi-insulating GaAs substrates with 2° toward (110) misorientation (closed circles) and 6° toward (111)B misorientation (open circles).

Figure 6 Electron concentration measured at 300K of n-GaInAsSb as a function of DETe mole fraction grown on (100) semi-insulating GaAs substrates with 2° toward (110) misorientation (closed circles) and 6° toward (111)B misorientation (open circles).

Figure 7 External quantum efficiency of GaInAsSb TPV devices grown on (100) GaSb substrates with 2° toward (110) misorientation (closed circles) and 6° toward (111)B misorientation (open circles).

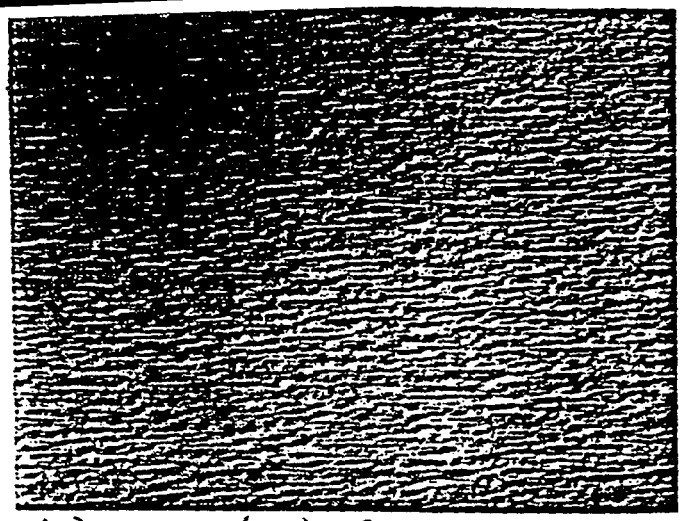

(a) (100) 2°→(110)

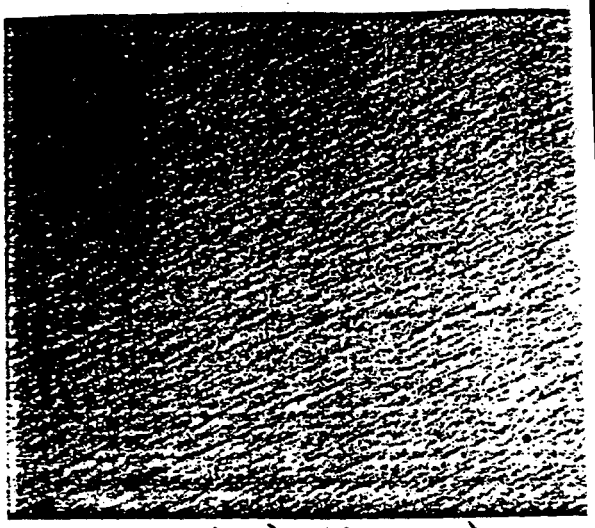

(b) (100) 6°→(110)

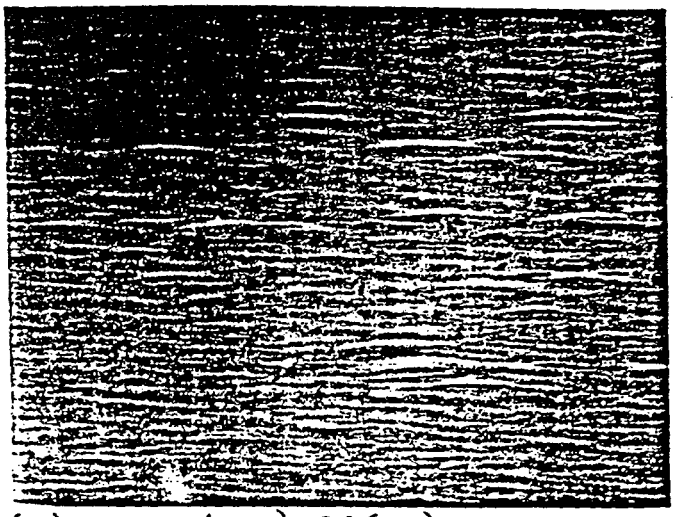

(c) (100) 2°(111)A

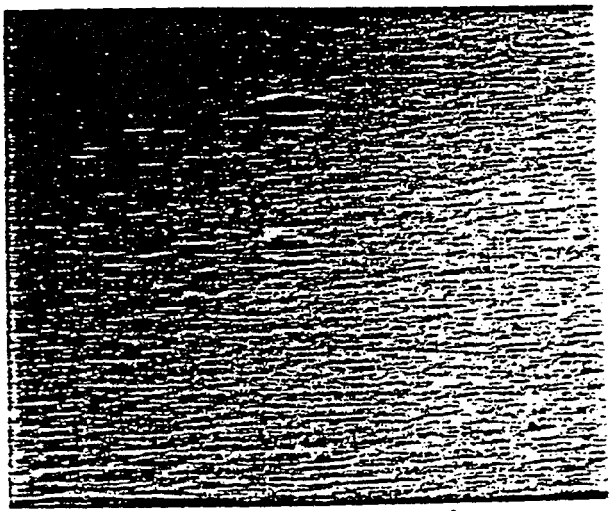

(d) (100) 6°→(111)A

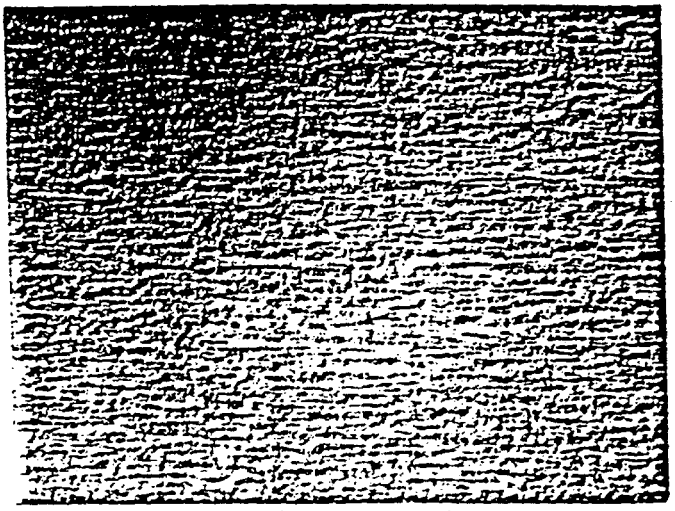

(e) (100) 2°→(111)B

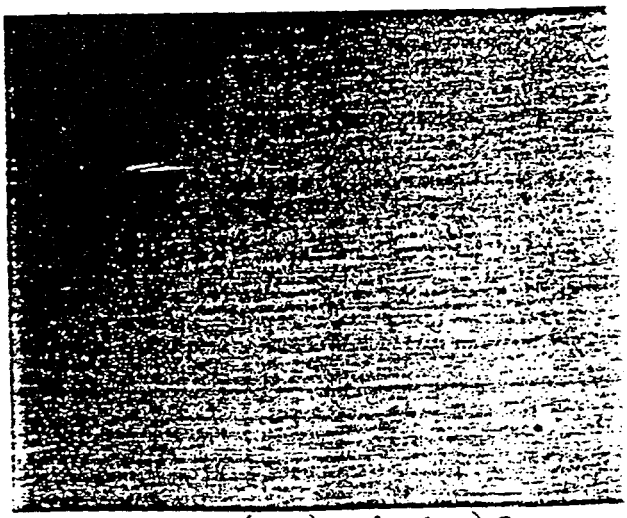

10 μm

(f) (100) 6°→(111)B

Figure 1

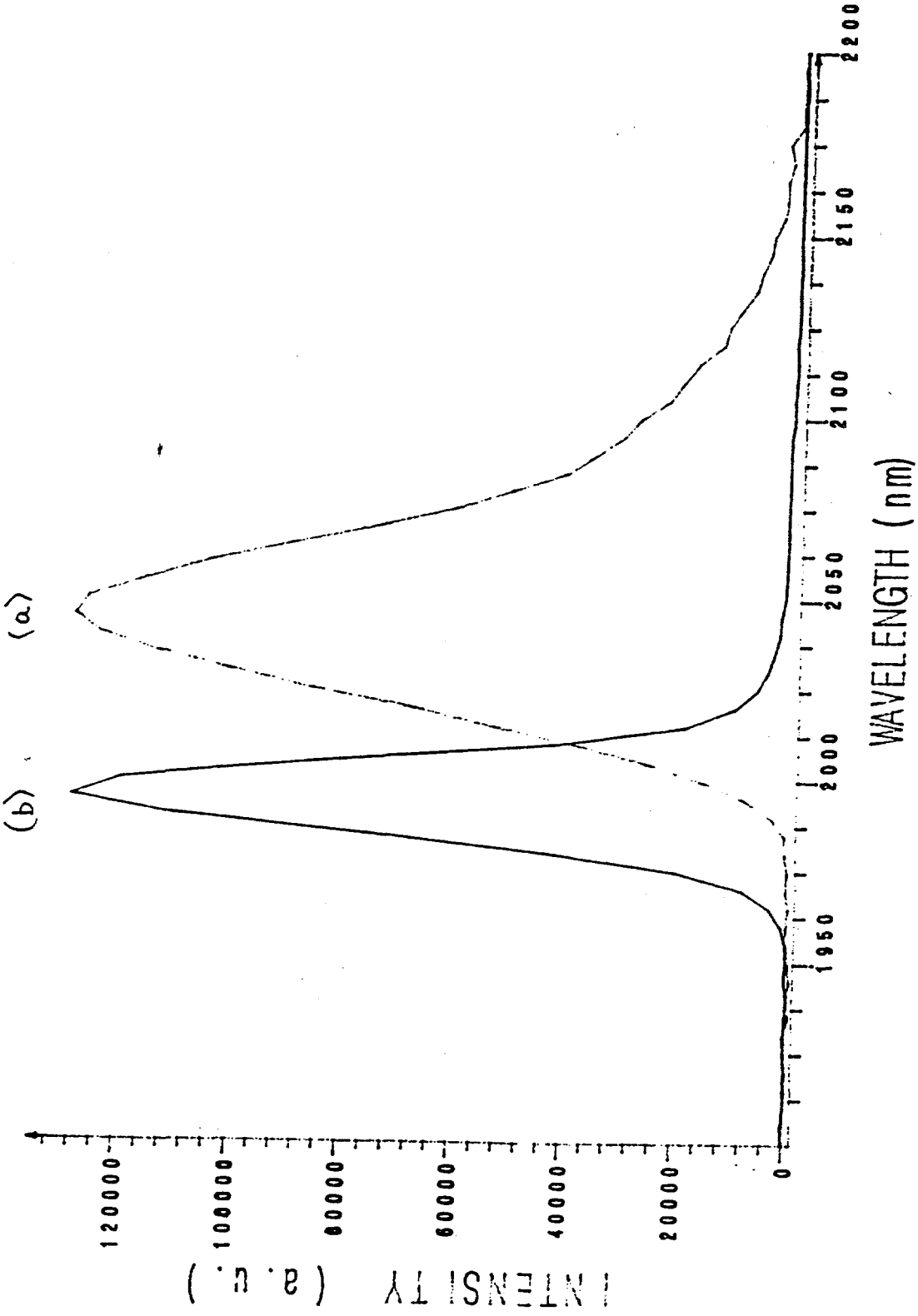

Figure 2

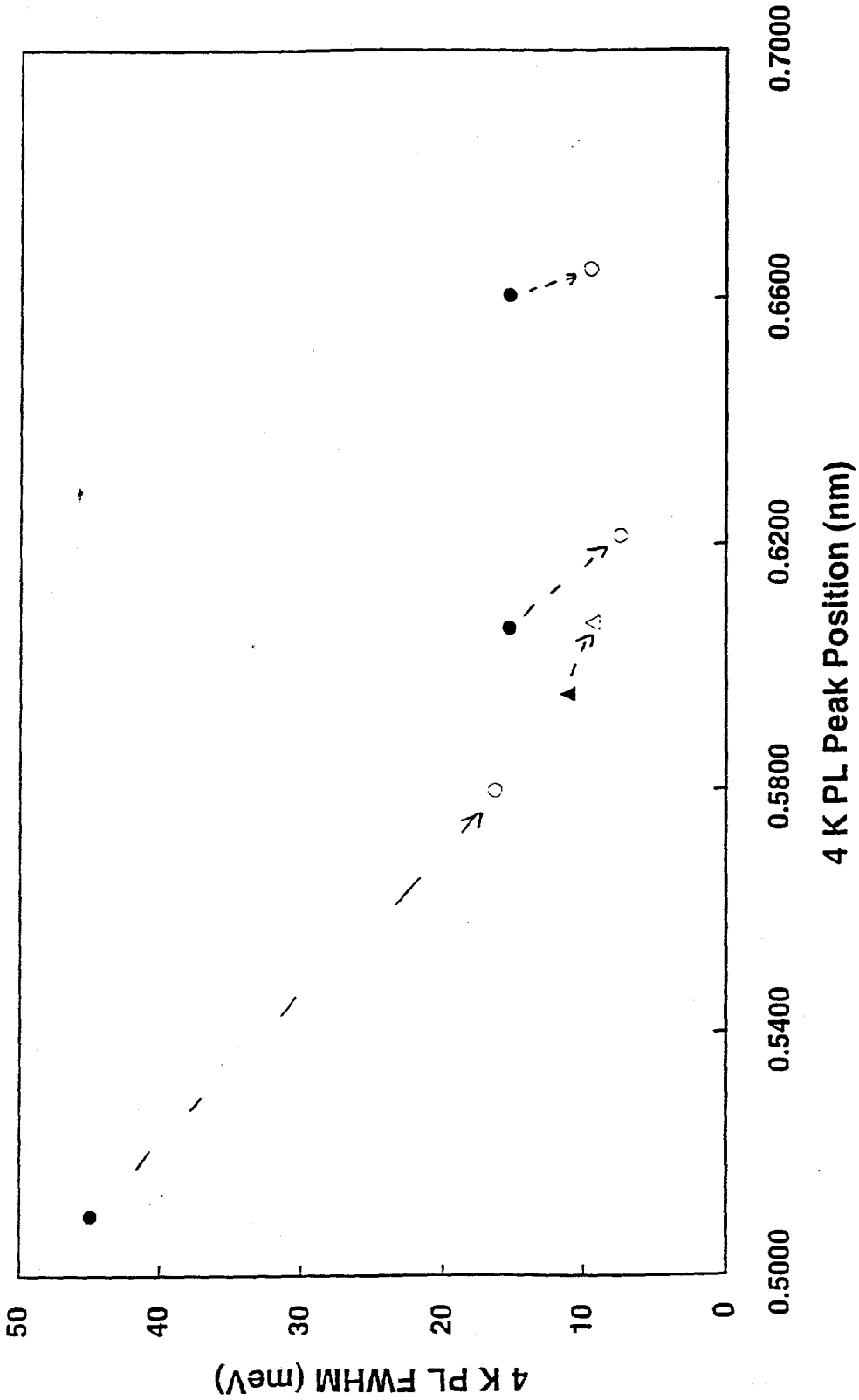

Figure 3

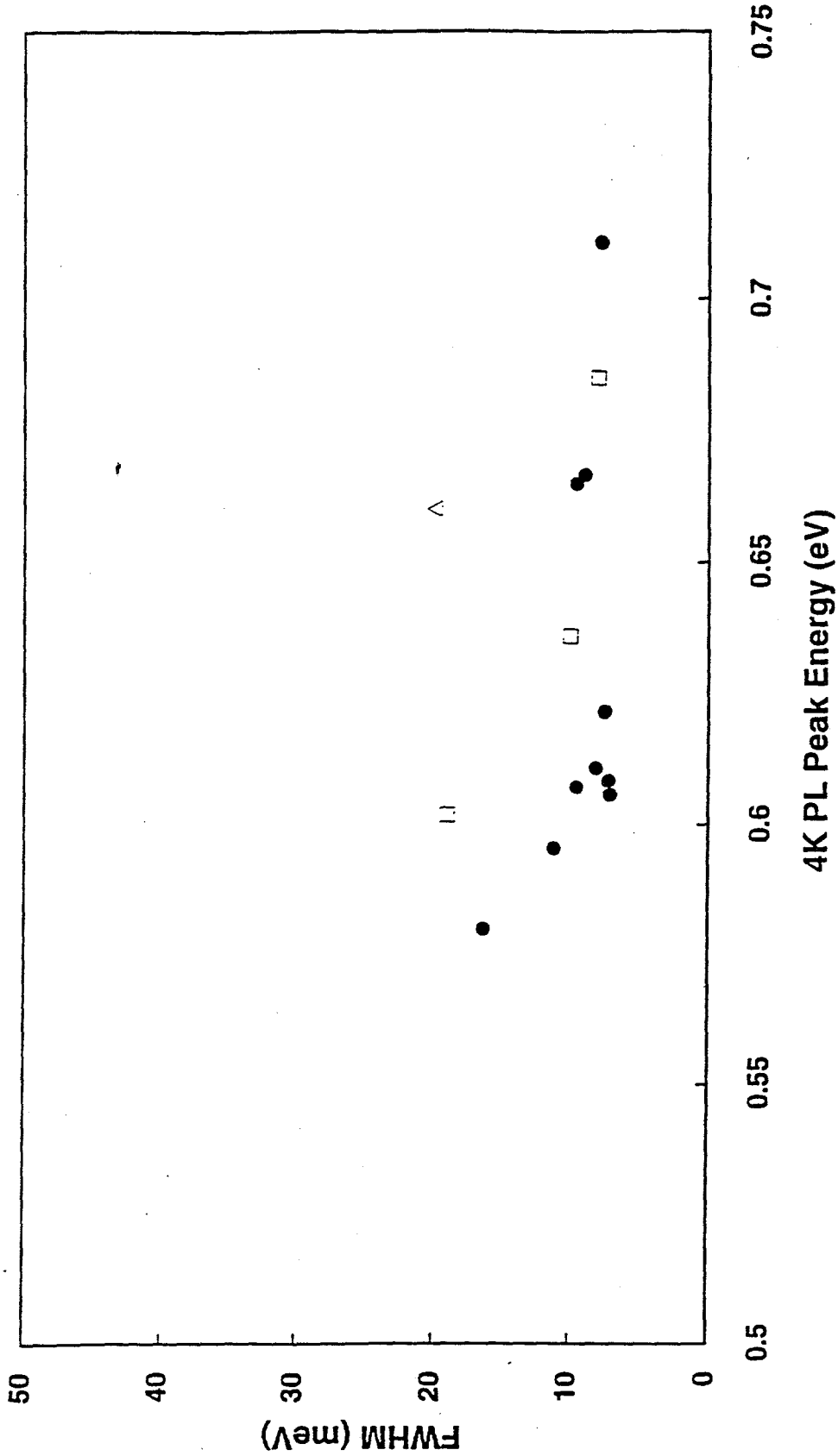

Figure 4

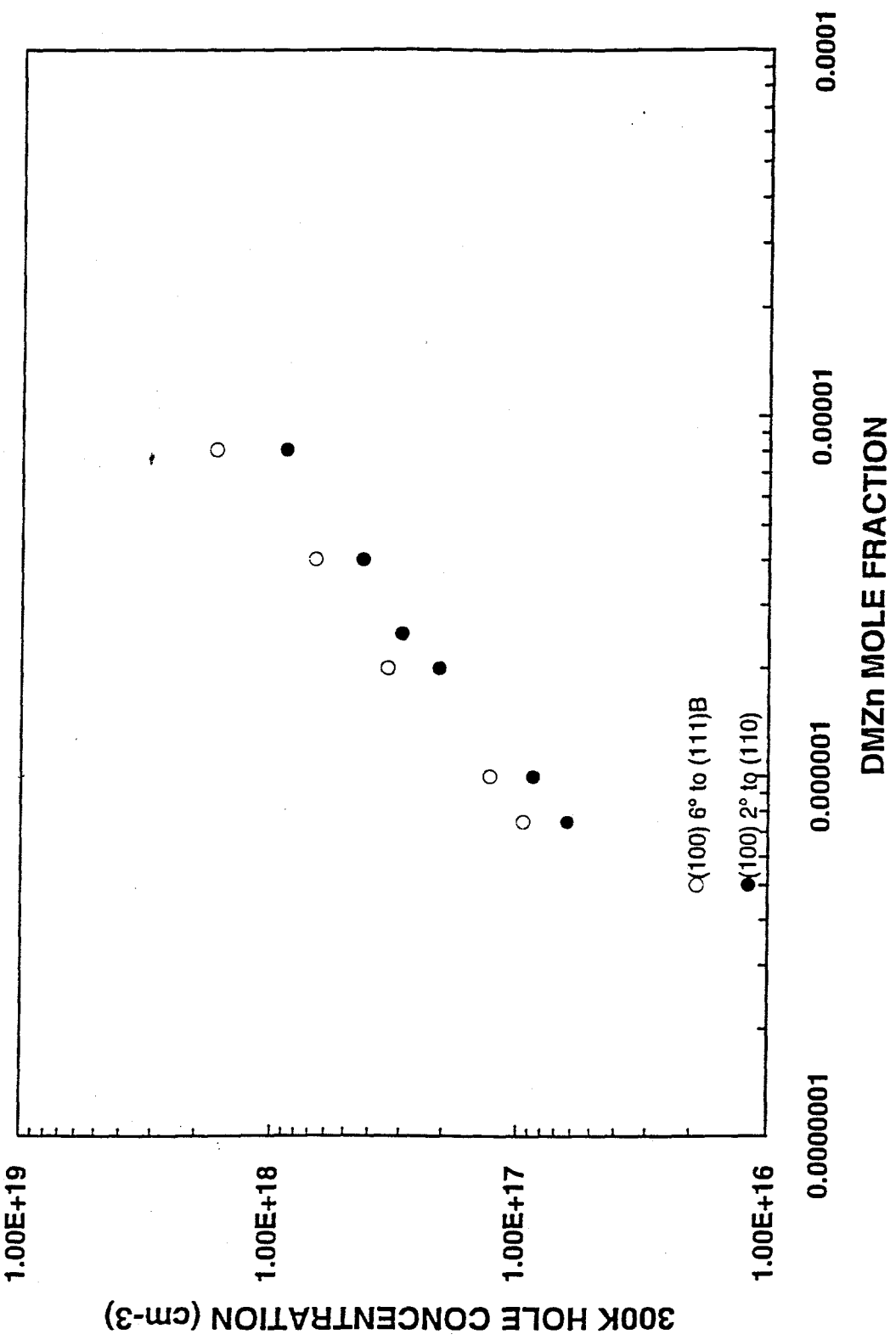

Figure 5

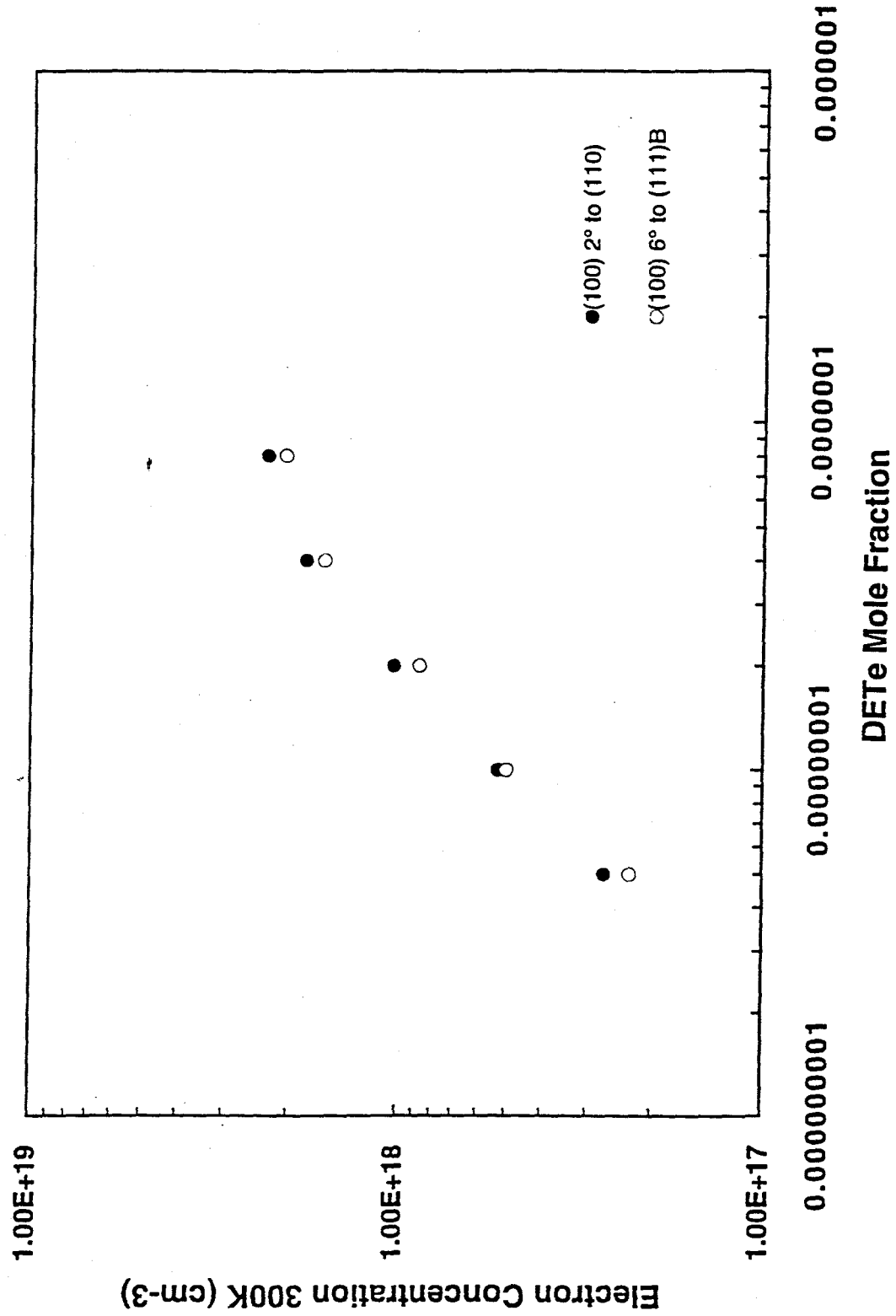

Figure 6

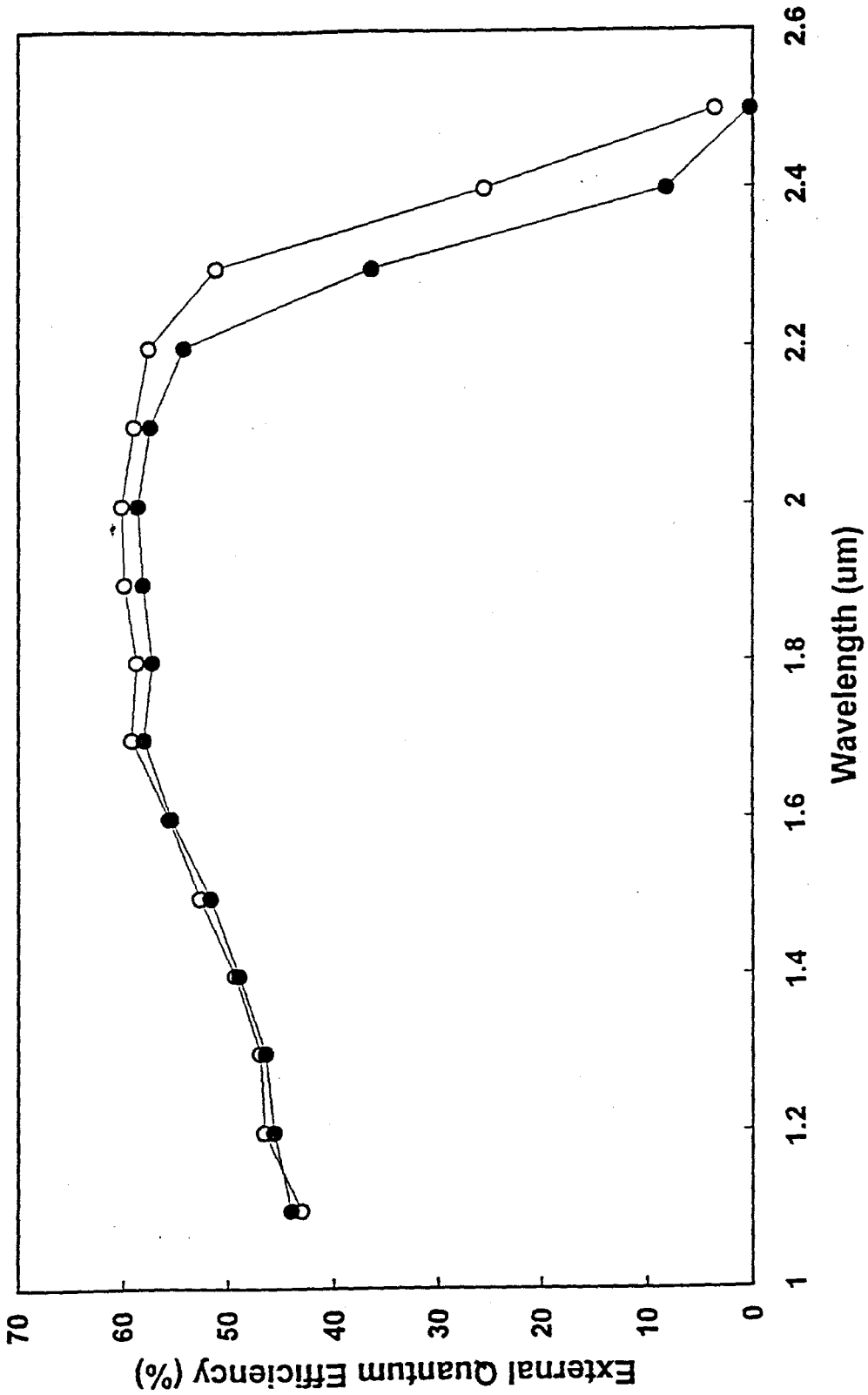

Figure 7